Biomedicine & Pharmacotherapy 86 (2017) 521–530

Available online at
ScienceDirect
www.sciencedirect.com

Elsevier Masson France
EM|consulte
www.em-consulte.com/en

Original article

Tetramethylpyrazine attenuates carbon tetrachloride-caused liver injury and fibrogenesis and reduces hepatic angiogenesis in rats

Shifeng Zhao[a], Zili Zhang[a], Linnan Qian[a], Qiuyi Lin[a], Chenxi Zhang[a], Jiangjuan Shao[b], Feng Zhang[a,c], Shizhong Zheng[a,c,*]

[a] Department of Pharmacology, College of Pharmacy, Nanjing University of Chinese Medicine, Nanjing 210023, PR China
[b] Department of Pharmacy, College of Pharmacy, Nanjing University of Chinese Medicine, Nanjing 210023, PR China
[c] Jiangsu Key Laboratory for Pharmacology and Safety Evaluation of Chinese Materia Medica, Nanjing University of Chinese Medicine, Nanjing, PR China

ARTICLE INFO

Article history:
Received 15 July 2016
Received in revised form 15 November 2016
Accepted 27 November 2016

Keywords:
Liver fibrosis
Tetramethylpyrazine
Liver sinusoidal endothelial cell
Capillarization
Angiogenesis
Apoptosis

ABSTRACT

Liver fibrosis represents a frequent event following chronic insult to trigger wound healing reactions with abnormalities of angiogenesis in the liver. Capillarization of liver sinusoidal endothelial cell (LSEC) is the pivotal event during liver angiogenesis. In the current study, we sought to investigate the effect of tetramethylpyrazine (TMP) on carbon tetrachloride (CCl_4)-induced liver injury and fibrosis in rats, and to further examine the molecular mechanisms of TMP-induced anti-angiogenic effect. We found that TMP significantly ameliorated histopathological feature of liver fibrosis characterized by decreased collagen deposition, hepatocyte apoptosis, and expression of biochemical indicators, such as aminotransferase (ALT), aspartate aminotransferase (AST) and alkaline phosphatase (ALP). Moreover, TMP appeared to play an essential role in controlling pathological angiogenesis. In addition, TMP attenuated angiogenesis by downregulation of vascular endothelial growth factor-A (VEGF-A), vascular endothelial growth factor receptor 2 (VEGF-R2), platelet-derived growth factor-BB (PDGF-BB), and platelet-derived growth factor-β receptor (PDGF-βR), four important factors transmitting pro-angiogenic pathways. Besides, TMP inhibited LSEC capillarization in CCl_4-induced liver fibrotic model with the morphological features of increasing sinusoidal fenestrae. Importantly, we found that disruption of angiogenesis is required for TMP to inhibit hepatocyte apoptosis in rats. Treatment with TMP significantly inhibited the expression of Bax, and up-regulated Bcl-2 expression. Interestingly, treatment with angiogenesis-inducer AngII dramatically eliminated the effect of TMP on Bax/Bcl-2 axis. Overall, these results provide novel perspectives to reveal the protective effect of TMP on liver, opening up the possibility of using TMP based anti-angiogenic drugs for the liver diseases.

1. Introduction

Liver fibrosis occurs as compensatory responses to tissue repairing process in a wide range of chronic liver injures, and angiogenesis is a typical feature of liver fibrosis [1]. Recent studies established a pivotal role for liver sinusoidal endothelial cells (LSECs) in liver angiogenesis because they play an important role in the parenchymal distribution of nutrients and oxygen, modulation of the hepatic vascular tone, blood pathogens clearance, and intrahepatic cells communication [2]. Endothelial cells form the wall of hepatic sinusoids and comprise approximately 16% of the cells in liver under physiological conditions [3]. The LSEC has a unique phenotype among all mammalian endothelial cells, LSEC have open fenestrae grouped into sieve plates and lack an organized basement membrane. The capillarization of LSEC is a key step in the pathogenesis of hepatic angiogenesis, which is characterized by formation of an organized basement membrane and lack of fenestration [4].

LSEC capillarization is also accompanied by overexpression of Platelet endothelial cell adhesion molecule-1 (PECAM-1/CD31), CD34 and von Willebrand factor (vWF), three markers of endothelial cells [5]. In addition, LSEC capillarization is also coupled with the sequential overexpression of platelet-derived growth factor (PDGF) [6], platelet-derived growth factor-β receptor (PDGF-βR) [7], vascular endothelial growth factor receptor 2 (VEGF-R2) [8], epidermal growth factor receptor (EGFR) [9] and hypoxia inducible factor 1α (HIF-1α) [10], which transmit

* Corresponding author at: Department of Pharmacology, College of Pharmacy, Nanjing University of Chinese Medicine, 138 Xianlin Avenue, Nanjing, Jiangsu 210023, PR China.
E-mail address: nytws@163.com (S. Zheng).

http://dx.doi.org/10.1016/j.biopha.2016.11.122
0753-3322/

the pro-angiogenesis VEGF, PDGF, and EGF pathways, respectively. Furthermore, chemical stimuli play a critical role in LSEC capillarization and angiogenesis [4]. Accumulating evidence demonstrated that capillarized LSECs not only preceded fibrosis, but also permitted for pathological sinusoidal angiogenesis, suggesting that inhibition of LSEC capillarization was a key step in anti-angiogenesis and restoration of liver functions [2].

Recently, new therapeutic agents and strategies are required for the management of anti-angiogenesis in liver fibrosis. The use of natural products as a realistic option for the treatment of liver fibrosis has broadly been accepted. Natural products are an important source of potential anti-angiogenic remedies. Chuanxiong has been widely used as one of a disease-preventing medicine throughout history. It has a variety of pharmacological activities including treatment of heart disease [11], fibrosis [12] as well as antibacterial [13]. Recent studies have shown that the extracts of Chuanxiong could protect the liver under a variety of pathological circumstances [14], but the evidence for hepatoprotection by a single Chuanxiong-derived component is rarely seen. We herein hypothesized that TMP contributed predominantly to the hepatoprotective effects by inhibiting the pathological angiogenesis. In this study, we sought to investigate the effect of TMP on carbon tetrachloride (CCl_4)-induced liver injury and fibrosis in rats, and to further examine the molecular mechanisms of TMP-induced anti-angiogenic effect.

2. Material and methods

2.1. Reagents and antibodies

TMP (purity >98%) and angiotensin-II (AngII) were purchased from Sigma (St Louis, MO, USA). Alzet osmotic pumps (models 2004 and 2ML4) were purchased from the Durect Corporation (Cupertino, CA, USA). Primary antibodies against α-SMA, α1(I) procollagen, and fibronectin were purchased from Epitomics (SanFrancisco, CA, USA). Primary antibodies against VEGF-A, VEGFR2, PDGF-BB, PDGF-Rβ, EGF, EGFR and HIF-1α were purchased from Santa Cruz Biotechnology (Santa Cruz, CA, USA). Primary antibodies against MMP2, MMP9, TIMP-1, TIMP-2, Cleaved Caspase-9, Bax, Bcl2, EGFR and β-actin were purchased from Cell Signaling Technology (Danvers, MA, USA). The horseradish peroxidase-conjugated secondary antibodies were purchased from Cell Signaling Technology (Danvers, MA, USA).

2.2. Animals and experimental design

Male Sprague–Dawley rats (180–220 g body weight) were obtained from Beijing Vital River Laboratory Animal Technology Co., Ltd. (Beijing, China). All animals were maintained at approximately 22 ± 2 °C and 55 ± 5% relative humidity, with a 12-h light: 12-h dark cycle, and had free access to laboratory chow and tap water. The experimental was approved by the institutional and local committee on the care and use of animals of Nanjing University of Chinese Medicine (Nanjing, China). All animals were cared for in accordance with the National Institutes of Health (USA) guidelines. A mixture of CCl_4 (0.1 ml/100 g body weight) and olive oil [1:1 (w/v)] was used to induce liver fibrosis in rats. After adaptive feed for a week, sixty-four rats were randomly divided into eight groups (eight rats per group) (Fig. 1A). Group 1 was the vehicle control in which rats were not administrated CCl_4 or TMP but intraperitoneally (i.p.) injected with olive oil. Group 2 was the CCl_4 group in which rats were i.p. injected with CCl_4 without TMP treatment. Groups 3 were treatment groups in which rats were i.p. injected with CCl_4 and orally given TMP at 100 mg/kg. Group 4 was the positive control in which rats were i.p. injected with CCl_4 and treated with colchicine (Yifeng Pharmacy, Nanjing, China). Group 5 was CCl_4 + saline group in which rats were i.p. injected with CCl_4 and continuous infusion of saline with mini-Osmotic pumps. Group 6 was the CCl_4 + AngII group in which rats were i.p. injected with CCl_4 and continuous infusion of AngII (25 μg/kg/h) with mini-Osmotic pumps. Group 7 was CCl_4 + TMP + saline group in which rats were i.p. injected with CCl_4, orally given TMP at 100 mg/kg and continuous infusion of saline with mini-Osmotic pumps. Group 8 was CCl_4 + TMP + AngII group in which rats were i.p. injected with CCl_4, orally given TMP at 100 mg/kg and continuous infusion of AngII with mini-Osmotic pumps. TMP and Colchicine (0.1 mg/kg) were suspended in sterile phosphate buffered saline (PBS) and given once daily by gavage during weeks 2–5. At the end of experiment, rats were sacrificed after being anesthetized by i.p. injection pentobarbital (50 mg/kg). Blood was collected, and livers were isolated and weighted quickly and stored at −80 °C until analysis.

2.3. Liver histopathology

Hematoxylin-eosin (HE) staining, sirius red collagen staining and masson-trichrome staining were performed as we previously described [15]. Representative views of liver sections were shown. All histopathological analyses were undertaken by an experienced histopathologist in a blinded manner.

2.4. Measurement of hepatic enzyme levels

Levels of alanine aminotransferase (ALT), aspartate aminotransferase (AST) and alkaline phosphatase (ALP) in serum samples were evaluated using enzyme-linked immunosorbent assay methods according to the kit protocols (Nanjing Jiancheng Bioengineering Institute, Nanjing, China). Experiments were performed in triplicate.

2.5. Determination of hepatic hydroxyproline

The hydroxyproline levels in the liver tissue and serum were determined using a kit (Nanjing Jiancheng Bioengineering Institute, Nanjing, China) according to the protocol. Briefly, three small pieces of liver tissues randomly excised from the liver of every rat were hydrolyzed in 6 N HCl at 110 °C for 24 h, and subsequently, they were neutralized with NaOH. Isopropanol in citrate acetate-buffered chloramine T was added to aliquots of the hydrolysate, followed by the addition of Ehrlich reagent. The chemical reaction occurred in the dark for 25 min at 60 °C. After centrifugation, absorbance of the supernatant of each sample was read at 558 nm using a 96-well plate spectrometer. *trans*-hydroxyproline was used as the standard for quantification. Values were normalized to the control. Experiments were performed in triplicate.

2.6. RNA isolation and real-time PCR

Total RNA was extracted from rat liver samples using Trizol reagent (Biouniquer Technology Co., Ltd, Nanjing, China) according to the manufacturer's protocol. Amplification kit was purchased from Bio-Rad Laboratories (Berkeley, CA, USA). Glyceraldehyde phosphate dehydrogenase (GAPDH) was used as the invariant control. All primers were obtained from GenScript (Piscataway, NJ, USA) and are listed as follows: α-SMA: (forward) 5′-CCGACCGAATGCAGAAGGA-3′, (reverse) 5′-ACAGAGTATTTGCGCTCCGGA-3′; α(I)Procollagen: (forward) 5′-CCTCAAGGGCTCCAACGAG-3′, (reverse) 5′-TCAATCACTGTCTTGCCCCA-3′; Fibronectin: (forward) 5′-TGTCACCCACCACCTTGA-3′, (reverse) 5′-CTGATTGTTCTTCAGTGCGA-3′; GAPDH: (forward) 5′-GGCCCCTCTGGAAAGCTGTG-3′; (reverse) 5′-CCGCCTGCTTCACCACCTTCT-3′. Results were from triplicate experiments.

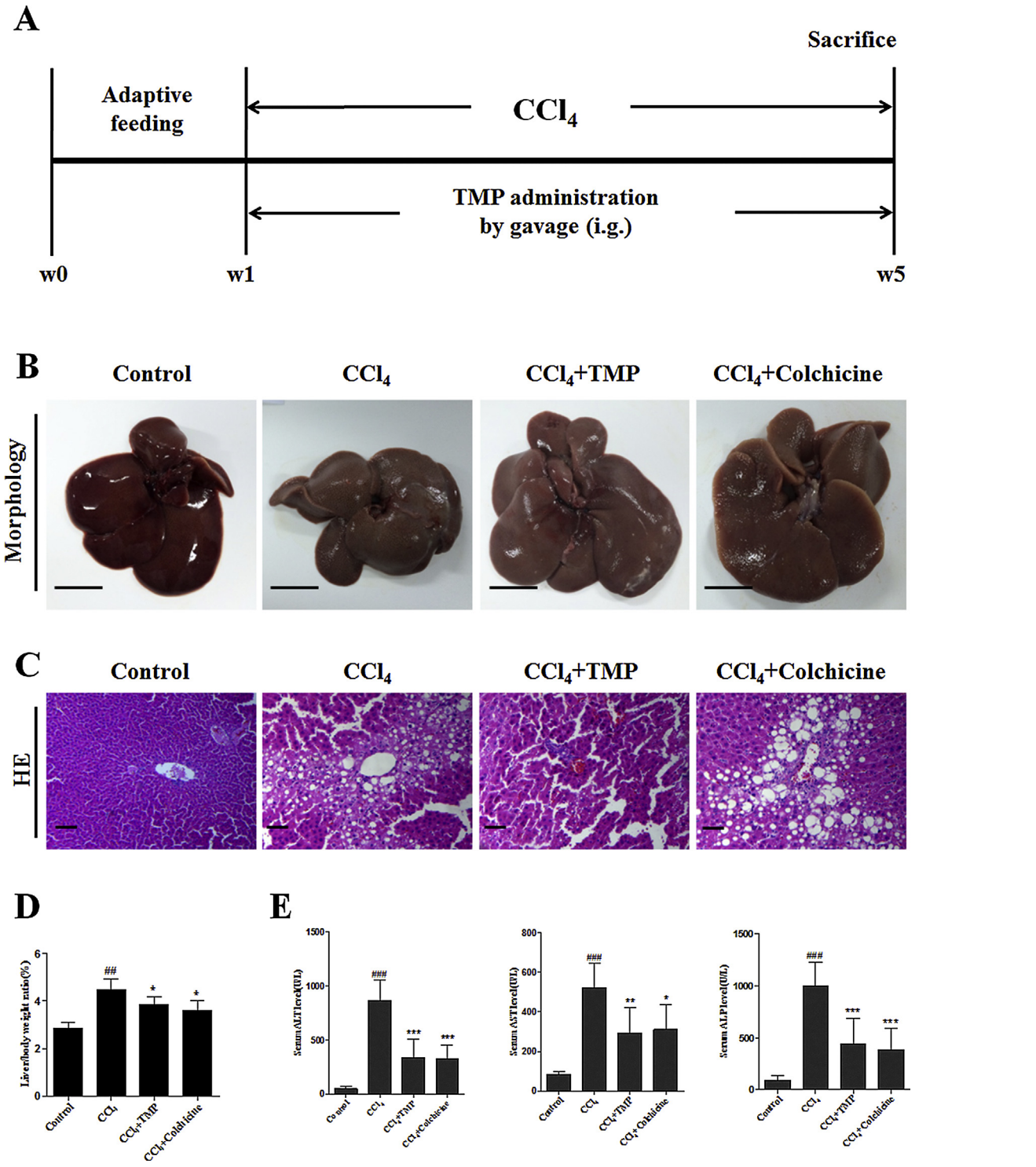

Fig. 1. TMP protects the rat liver from CCl_4-induced injury. Rats were grouped as follows: control group, no CCl_4, no treatment; CCl_4 group, with CCl_4, no treatment; CCl_4 + TMP group, TMP (100 mg/kg) and CCl_4-treated group; CCl_4 + colchicine group, colchicine (0.1 mg/kg) and CCl_4-treated group. **(A)** Scheme of the animal experiments. **(B)** Gross examination of rat livers. Representative photographs are shown. Scale bar = 1 cm. **(C)** Liver sections were stained with HE for histological examination. Representative photographs are shown. Scale bar = 20 μm. **(D)** Calculation of the rat liver/body weight ratio. **(E)** Determination of serum ALT, AST, ALP levels. Data are expressed as mean ± SD (n = 8/group); $^{\#\#}p < 0.01$ versus control group, $^{\#\#\#}p < 0.001$ versus control group, $^{*}p < 0.05$ vs. group 2, $^{**}p < 0.01$ versus CCl_4 group, $^{***}p < 0.001$ versus CCl_4 group.

2.7. Western blot analysis

Liver samples were homogenized in radio-immunoprecipitation assay (RIPA) buffer containing protease inhibitors. The protein levels were determined using a bicinchoninic acid (BCA) assay kit (Pierce, USA). Proteins (50 μg/well) were separated by sodium dodecyl sulfate (SDS)-polyacrylamide gel, transferred to a poly (vinylidene fluoride) (PVDF) membrane (Millipore, Burlington, MA,

USA), blocked with 5% skim milk in Tris-buffered saline containing 0.1% Tween 20. Target proteins were detected by corresponding primary antibodies and subsequently by horseradish peroxidase-conjugated secondary antibodies. Protein bands were visualized using a chemiluminescence reagent (Millipore, Burlington, MA, USA). Equivalent loading was confirmed using an antibody against β-actin. The levels of target protein bands were densitometrically determined using Quantity One 4.4.1. The variation in the density of bands was expressed as fold changes compared to the control in the blot after being normalized to β-actin. Representative blots were from three independent experiments.

2.8. Enzyme-linked immunosorbent assay (ELISA)

The levels of VEGF-A and PDGF-BB in liver tissues and serum were determined using an ELISA kit (Shanghai MLBIO Biotechnology Co. Ltd, Shanghai, China) according to the protocol. Eight duplicate wells were set up for each group. Results were from triplicate experiments.

2.9. Scanning electron microscopic (SEM) analysis

After the Rat was sacrificed, the livers were isolated and weighted quickly after killed. The livers were then collected and cut into small blocks, which were then fixed in 4% osmium for 1 h. The livers were then processed for sequential alcohol dehydration and infiltrated with t-butyl alcohol. After freezing, the tissues were vacuum-dried and then coated with ion sputter Hitachi E-1030 (Hitachi, Tokyo, Japan) for analysis with the scanning electron microscope SEM S-4100 (Hitachi). For quantification of fenestrae in liver sinusoids, the number of fenestrae (per μm^2) was analyzed with ImageJ (NIH, Bethesda, Maryland, USA) [16].

2.10. Immunofluorescence staining

Immunofluorescence staining with liver tissues was performed as we previously reported [7]. 4′, 6-Diamidino-2-phenylindole (DAPI) was used to stain the nucleus in liver tissues.

2.11. TUNEL staining analysis

Liver tisues of rat were stained with the TUNEL reagents using a staining kit (Nanjing KeyGEN Biotechnology CO., Ltd., Nanjing, China) according to the protocols. Morphology of apoptotic cells was photographed using a fluorescence microscope (Nikon, Tokyo, Japan) in a blinded fashion at random fields. Representative views of liver sections are shown.

2.12. Statistical analysis

Data were presented as mean ± SD and analyzed using SPSS16.0 software. Significance of difference was determined by one-way ANOVA with post-hoc Dunnett's test. Values of $p < 0.05$ were considered to be statistically significant.

3. Results

3.1. TMP protects rat liver from CCl_4-induced injury

We initially examined the ameliorative effects of TMP on hepatic injury in male Sprague-Dawley rats induced by CCl_4. Gross examination showed that morphological changes pathologically occurred in the rat liver with CCl_4 injection compared to the normal liver, but treatment with TMP improved the pathological changes in livers, and colchicine as a positive control also effectively protected the rat liver from CCl_4-induced injury (Fig. 1**B**). TMP and colchicine also significantly reduced the liver/body weight ratio, which was significantly elevated by CCl_4 injection (Fig. 1**B**, **D**). H&E staining further showed that TMP treatment resulted in remarkable improvement in liver histology evidenced by the ameliorated state of liver steatosis, necrosis, and fibrotic septa in the liver (Fig. 1**C**). Colchicine also significantly improved liver histology similar to TMP (Fig. 1**C**). ALT, AST and ALP are three well-established biomarkers for hepatocyte injury. Our data demonstrated that TMP and colchicine reduced serum levels of ALT, AST and ALP in CCl_4-treated rats (Fig. 1**E**). Taken together, these data suggested that TMP prevented hepatic injury caused by CCl_4 injection.

3.2. TMP reduces CCl_4-induced extracellular matrix deposition in rat liver

Excessive extracellular matrix (ECM) deposition leads to fibrogenesis during chronic liver injury and collagen is the main component of ECM. Therefore, we used Sirius red staining and Masson staining to examine the status of collagen expression in the rat liver, showing that collagens were severely deposited in the CCl_4-induced liver injury accompanied by nodular formation, but were reduced in the liver of rats treated with TMP (Fig. 2**A**). In addition, hydroxyproline is a unique amino acid composition of collagen, and its abundance in the liver reflects the changes in collagen metabolism [17]. Determination of hepatic hydroxyproline showed that its content in the fibrotic liver was significantly decreased by TMP and colchicine, indicating reduced collagen accumulation in the fibrotic liver (Fig. 2**B**). Real time-PCR and western blot assay showed significantly increased expression of α-SMA, α1 (I) procollagen, fibronectin at both mRNA and protein levels, indicating excessive deposition of ECM in the fibrotic liver (Fig. 2**C**, **D**). However, treatment with TMP diminished their gene and protein expression, and colchicine also produced a potent inhibitory effect on collagen expression (Fig. 2**C**, **D**). Collectively, these data suggested that TMP could attenuate CCl_4-induced liver fibrogenesis by inhibiting collagen expression in rats.

3.3. TMP attenuates angiogenesis in CCl_4-caused fibrotic liver in rats

Angiogenesis plays a critical role in damaging the liver and promoting hepatic fibrogenesis resulting from the metabolism of CCl_4 in the liver [7]. ELISA assay was used to determine the expression of VEGF-A and PDGF-BB in liver homogenate and serum. Administration of CCl_4 significantly increased the liver and serum levels of VEGF-A and PDGF-BB, but treatment with TMP and colchicine decreased their levels (Fig. 3**A**, **B**). In addition, western blot assay showed significantly increased expression of VEGF-A, VEGF-R2, PDGF-BB, PDGF-Rβ, EGF, EGFR as well as HIF-1α at protein levels in CCl_4-treatment rats, indicating excessive angiogenesis in the fibrotic liver, but the levels of these factors were significantly diminished in TMP and colchicine administered rats (Fig. 3**C**). Furthermore, base membrane was a special structure which embraces vascular endothelial cells, but was deficiency in hepatic sinusoids. It should be noted that matrix metalloproteinase (MMP) −2, MMP-9 two key factors for matrix regression, and matrix metalloproteinase inhibitor (TIMP) −1, TIMP-2 two factors inhibiting the regression of matrix plays an very important roles in angiogenesis [1,7]. Western blot assay showed TMP significantly increased expression of TIMP-1, TIMP-2 and decreased expression of MMP-2, MMP-9 at protein levels, and indicating excessive basement membrane in the fibrotic liver (Fig. 3**D**). However, treatment with colchicine also produced a potent inhibitory effect on collagen expression evidenced (Fig. 3**D**). Altogether, these data

revealed that TMP attenuated angiogenesis in the rat fibrotic liver caused by CCl_4 administration.

3.4. TMP inhibits LSEC capillarization in CCl_4-caused fibrotic liver in rats

As the main cell involved in liver angiogenesis, LSEC capillarization plays a key role in pathological angiogenesis. We determined the LSEC capillarization marker in the rat liver using different methods. Firstly, we used high-performance scanning electron microscopy (SEM) to investigate whether TMP decreased any morphological changes in the liver. Sieve plate structures (fenestrae) were present in the liver sinusoids of normal rats (arrow), but were not present in CCl_4-induced models (Fig. 4**A**). On the contrary, fenestration was recurred in both treatment with TMP and colchicine (Fig. 4**A**). We additionally used immunofluorescence double staining to further validate capillarized LSEC on hepatic fibrosis. Similar results indicated that the elevated expression of liver fibrosis maker was abrogated by TMP concomitant with decreased CD31 positive cells in CCl_4-induced rat liver (Fig. 4**B**). In addition, western blot assay showed significantly increased expression of CD31, CD34, vWF at protein levels in CCl_4-induced fibrosis model, indicating excessive LSEC capillarization in the fibrotic liver. However, treatment with TMP diminished their mRNA and protein expression, and colchicine also significantly inhibited their expression in the rat fibrotic liver

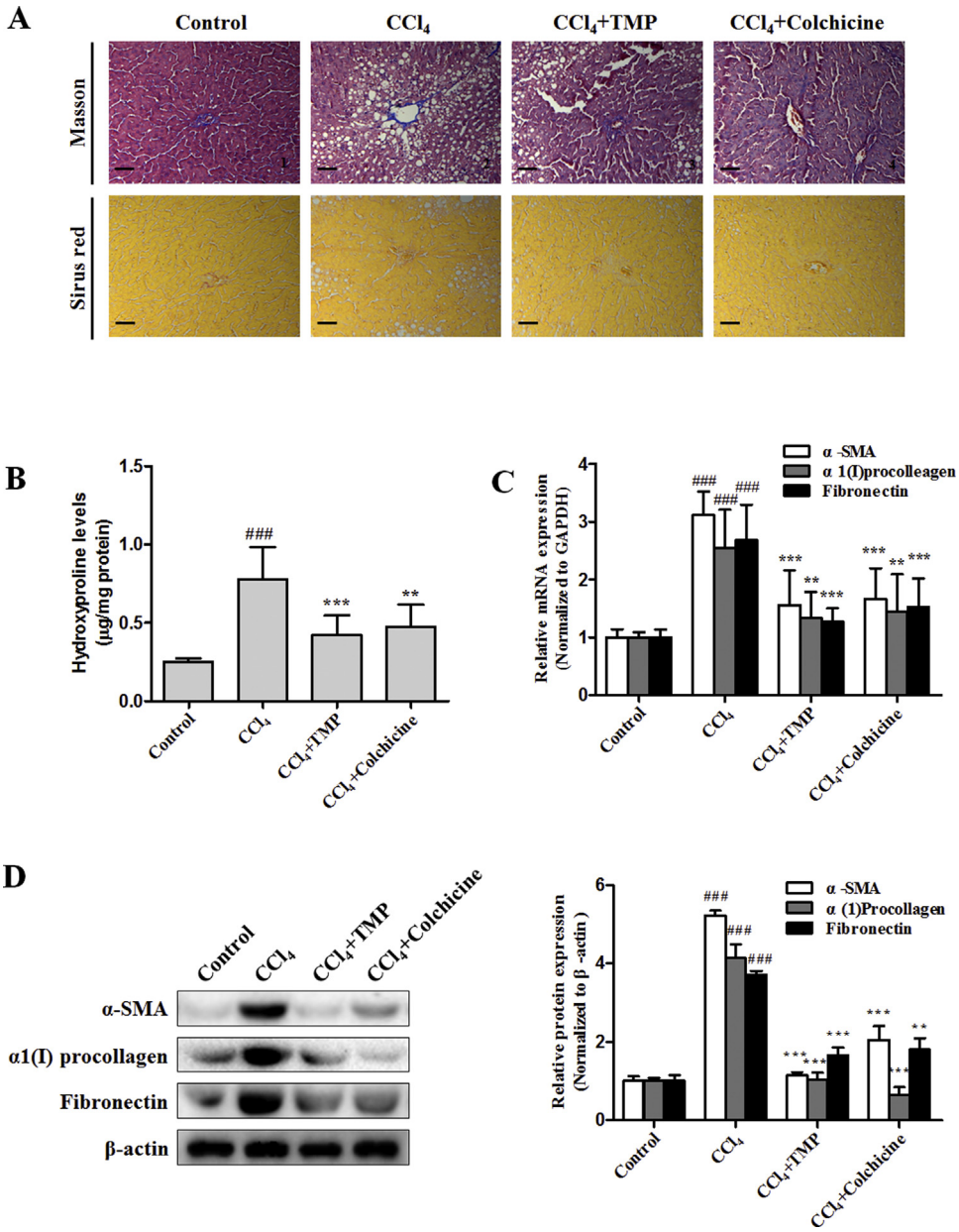

Fig. 2. TMP reduces CCl_4-induced extracellular matrix deposition in the rat liver. Rats were grouped as follows: control group, no CCl_4, no treatment; CCl_4 group, with CCl_4, no treatment; CCl_4 + TMP group, TMP (100 mg/kg) and CCl_4-treated group; CCl_4 + colchicine group, colchicine (0.1 mg/kg) and CCl_4-treated group. **(A)** Masson and Sirius red staining of collagens in liver tissues. Scale bar = 20 μm. **(B)** Determination of the hydroxyproline content in the liver homogenate. **(C)** Real time-PCR analyses of α-SMA, α1(I) procollagen, fibronectin. GAPDH was used as the invariant control. **(D)** Western blot analyses of α-SMA, α1 (I) procollagen, fibronectin. β-actin was used as an invariant control for equal loading. Representative blots are shown with densitometry. Data are expressed as mean ± SD (n = 8/group); $^{###}p < 0.001$ versus control group, $^{*}p < 0.05$ versus CCl_4 group, $^{**}p < 0.01$ versus CCl_4 group, $^{***}p < 0.001$ versus CCl_4 group.

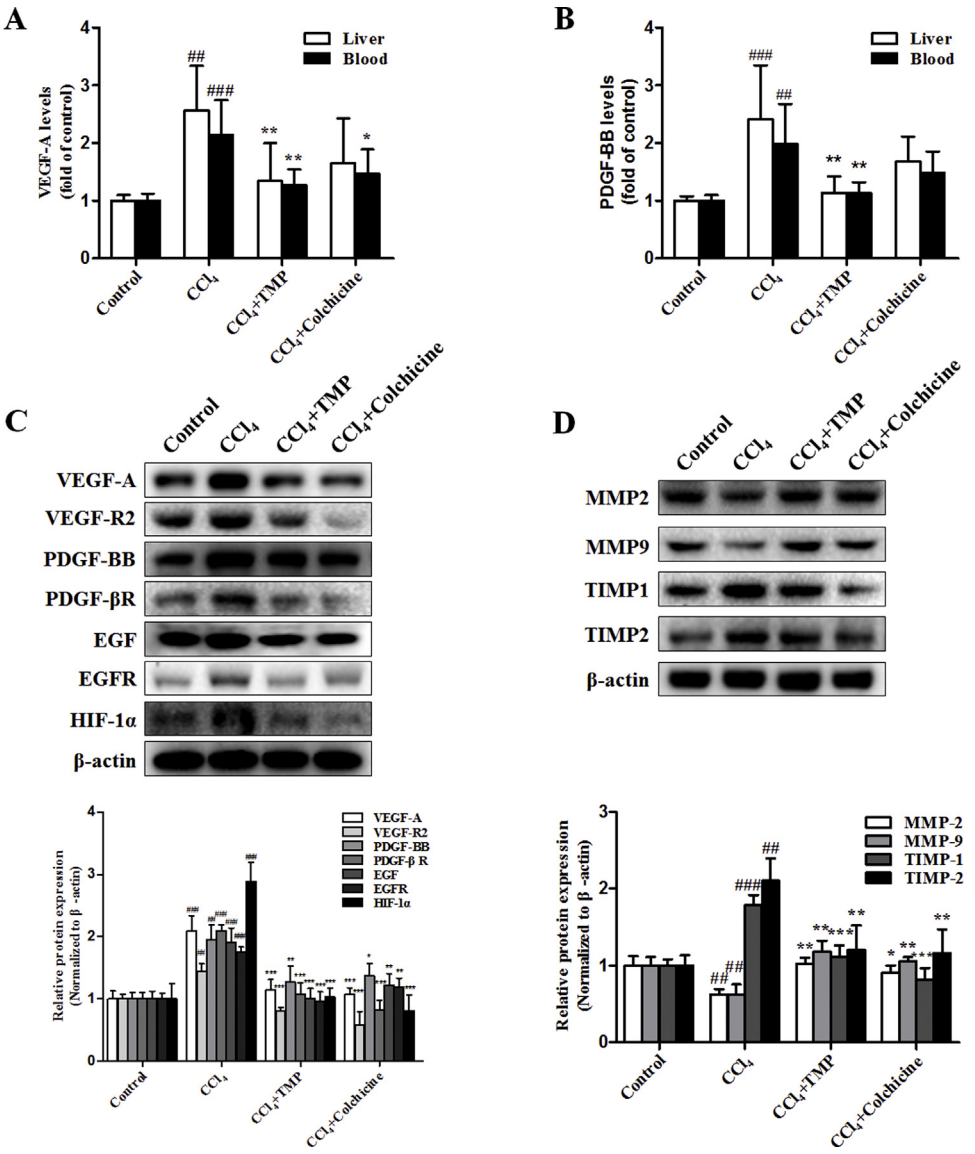

Fig. 3. TMP attenuates angiogenesis in the CCl_4-caused fibrotic liver in rats. Rats were grouped as follows: control group, no CCl_4, no treatment; CCl_4 group, with CCl_4, no treatment; CCl_4 + TMP group, TMP (100 mg/kg) and CCl_4-treated group; CCl_4 + colchicine group, colchicine (0.1 mg/kg) and CCl_4-treated group. **(A)** Determination of liver homogenate and serum VEGF-A levels. **(B)** Determination of liver tissue and serum PDGF-BB levels. **(C)** Western blots analyses of VEGF-A, VEGF-R2, PDGF-BB, PDGF-βR, EGF and EGFR. β-actin was used as an invariant control for equal loading. Representative blots are shown with densitometry. **(D)** Western blot analyses of MMP-2, MMP-9, TIMP-1, TIMP-2. β-actin was used as an invariant control for equal loading. Representative blots are shown with densitometry. Data are expressed as mean ± SD (n = 8/group), $^{\#\#}p < 0.01$ versus control group, $^{\#\#\#}p < 0.001$ versus control group, $^{*}p < 0.05$ versus CCl_4 group, $^{**}p < 0.01$ versus CCl_4 group, $^{***}p < 0.001$ versus CCl_4 group.

(Fig. 4**C**). Collectively, these results indicated that TMP inhibited LSEC capillarization in CCl_4-caused fibrotic liver in rats.

3.5. Disruption of angiogenesis is required for TMP to inhibit hepatocyte apoptosis in rats

Since apoptosis contributed to progressive liver remodeling and dysfunction after liver fibrosis, we subsequently explored whether blockade of sinusoidal angiogenesis contributed to TMP-induced inhibition of hepatocyte apoptosis. On the one hand, we examined the effects of TMP on apoptosis in the liver tissues by TUNEL staining. The level of hepatocyte apoptosis (arrow) was decreased significantly after treatment with TMP compared to CCl_4-induced group (Fig. 5**A**). On the other hand, the key factors of apoptosis such as Bax, Bcl-2, cleaved caspase-9 and cleaved poly ADP-ribose polymerase (PARP) were also examined by western blot to clarify the potential mechanisms. The expression of pro-apoptotic protein Bax was significantly up-regulated while that of anti-apoptotic protein Bcl-2 was significantly down-regulated in the CCl_4 treated group compared to those of the control group. Treatment with TMP significantly reversed the dysregulated expressions of Bax and Bcl-2 (Fig. 5**B**). Moreover, the expressions of Cleaved Caspase-9 and Cleaved PARP, the other two apoptosis markers, were also increased significantly in the CCl_4 treated group (Fig. 5**B**). In contrast, TMP significantly inhibited the expressions of such two proteins. Importantly, we used AngII as an angiogenesis inducer to impire the disruption of angiogenesis by TMP, and in turn determined the change of hepatocyte apoptosis. The present results have demonstrated that AngII significantly promoted angiogenesis characterized by increased VEGF-A, PDGF-BB, VEGF-R2, PDGF-βR and HIF-1α expression (Fig. 5C–E). Besides, we found that treatment with TMP significantly inhibited the expression of Bax (Fig. 5**F**), and up-regulated the expression of Bcl-2 at protein levels (Fig. 5**F**). Interestingly, AngII treatment dramatically eliminated the effect of TMP on Bax/Bcl-2 axis (Fig. 5**F**). Moreover, the expressions of Cleaved Caspase-9 and

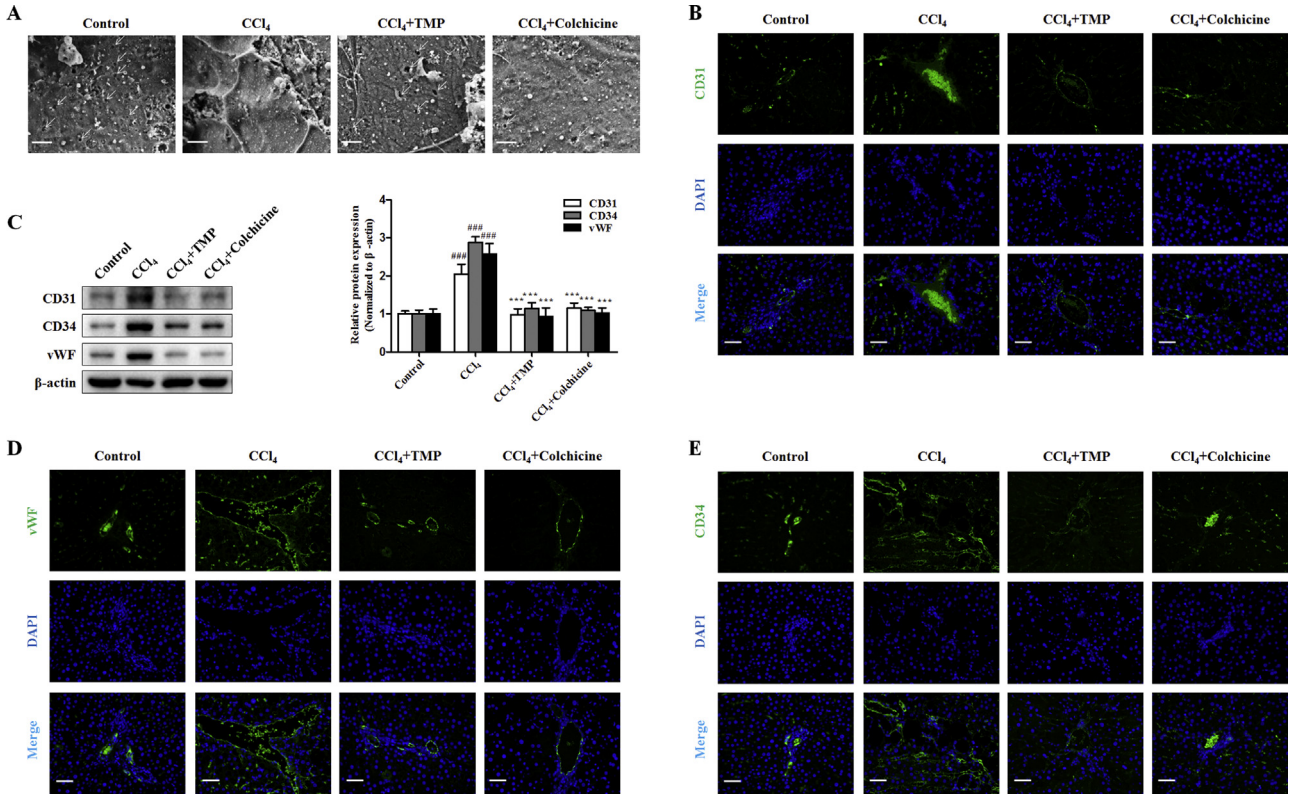

Fig. 4. TMP inhibits LSEC capillarization in the CCl_4-caused fibrotic liver in rats. Rats were grouped as follows: control group, no CCl_4, no treatment; CCl_4 group, with CCl_4, no treatment; CCl_4 + TMP group, TMP (100 mg/kg) and CCl_4-treated group; CCl_4 + colchicine group, colchicine (0.1 mg/kg) and CCl_4-treated group. **(A)** LSEC sieve plates (arrow) were examined by SEM at 5000 magnification. The pictures shown for each treatment group represent one picture selected from a total of eight representative images. Scale bar = 1 μm. **(B)** Liver sections were stained with immunofluorescence by using antibodies against CD31 (green) and α-SMA (red). Representative photographs are shown. Scale bar = 20 μm. **(C)** Western blot analyses of CD31, CD34, vWF. β-actin was used as an invariant control for equal loading. Representative blots are shown with densitometry. Data are expressed as mean ± SD (n = 8/group); $^{###}p < 0.001$ versus control group, $^{***}p < 0.001$ versus CCl_4 group.

Cleaved PARP were also down-regulated by TMP treatment, while AngII treatment impaired the inhibition of TMP (Fig. 5**F**). This result was confirmed by immunofluorescence staining with Cleaved Caspase-9 and Cleaved PARP antibody (Fig. 5**G**, **H**). These findings collectively suggested that disruption of apoptotic signaling was required for TMP exerted liver-protective effects on CCl_4-induced liver angiogenesis and fibrosis.

4. Discussion

Currently, the treatments of liver fibrosis are mainly through drug therapy, interventional therapy, rehabilitation therapy and routine therapy. Unfortunately, the therapeutic effect is unsatisfactory, and patients often suffer from severe and persistent pain or even death. Thus, it is of great significance to explore the pathogenesis of liver fibrosis and to find effective medications.

TMP, a botanical compound derived mainly from the rhizome of Chuanxiong, has been widely used in traditional medicine. A series of reports highlighted its benefits in cardioprotection [18], neuroprotection [19], and immune regulation [20]. In the current study, we evaluated the antifibrotic efficacy of TMP in a classical animal model of liver fibrosis. Liver fibrosis induced by CCl_4 has been extensively used in experimental models in rats because hepatic responses in rats to chronic CCl_4 insult are shown to be superficially similar to human liver fibrosis [21]. We herein demonstrated that TMP effectively improved liver histology, decreased serum levels of hepatic enzymes, and inhibited collagen production in the rat liver with injury and fibrogenesis caused by CCl_4. These findings were consistent with previous *in vivo* evidence that the extracts of Chuanxiong protected the liver from damages caused by CCl_4 [15,22] and Dimethyl ammonium nitrite [23] in rodents. Furthermore, we herein selected colchicine as a positive control for evaluation of TMP, because colchicine has been sufficiently demonstrated to be a natural hepatoprotective agent via anti-inflammatory, antifibrotic, and immunomodulatory effects in a large number of basic and clinical investigations, despite a recent notion that colchicine should not be used for liver fibrosis or cirrhosis irrespective of the etiology [24]. The dose of colchicine was set referring to previous reports showing that colchicine at 0.1 mg/kg was effective in inhibiting collagen synthesis and improving liver fibrosis [25]. In the present study, we found that TMP at 100 mg/kg produced protective effects on the rat liver comparable to that of colchicine in many assessments. More importantly, recent studies have shown that TMP can protect various organs against toxicity. Guan D., et al. reported that TMP could inhibit $CoCl_2$-induced neurotoxicity through enhancement of Nrf2/GCLc/GSH and suppression of HIF1α/NOX2/ROS pathways [26], Sun X.C., et al. reported that TMP could against cisplatin induced ototoxicity in guinea pigs. Our present research shows that TMP could alleviate liver injury induced by CCl_4 intoxication [27].

Angiogenesis has a pivotal role in the formation of portal-systemic shunts. Recent research has defined that many of the mediators and mechanisms were involved in this angiogenic process, linking the central role of liver sinusoidal endothelial cells capillarization. Studies of animal models have demonstrated the potential therapeutic impact of drugs to inhibit angiogenesis in cirrhosis, portal hypertension, portal-systemic collaterals contribute to circulatory disturbance, gastrointestinal hemorrhage,

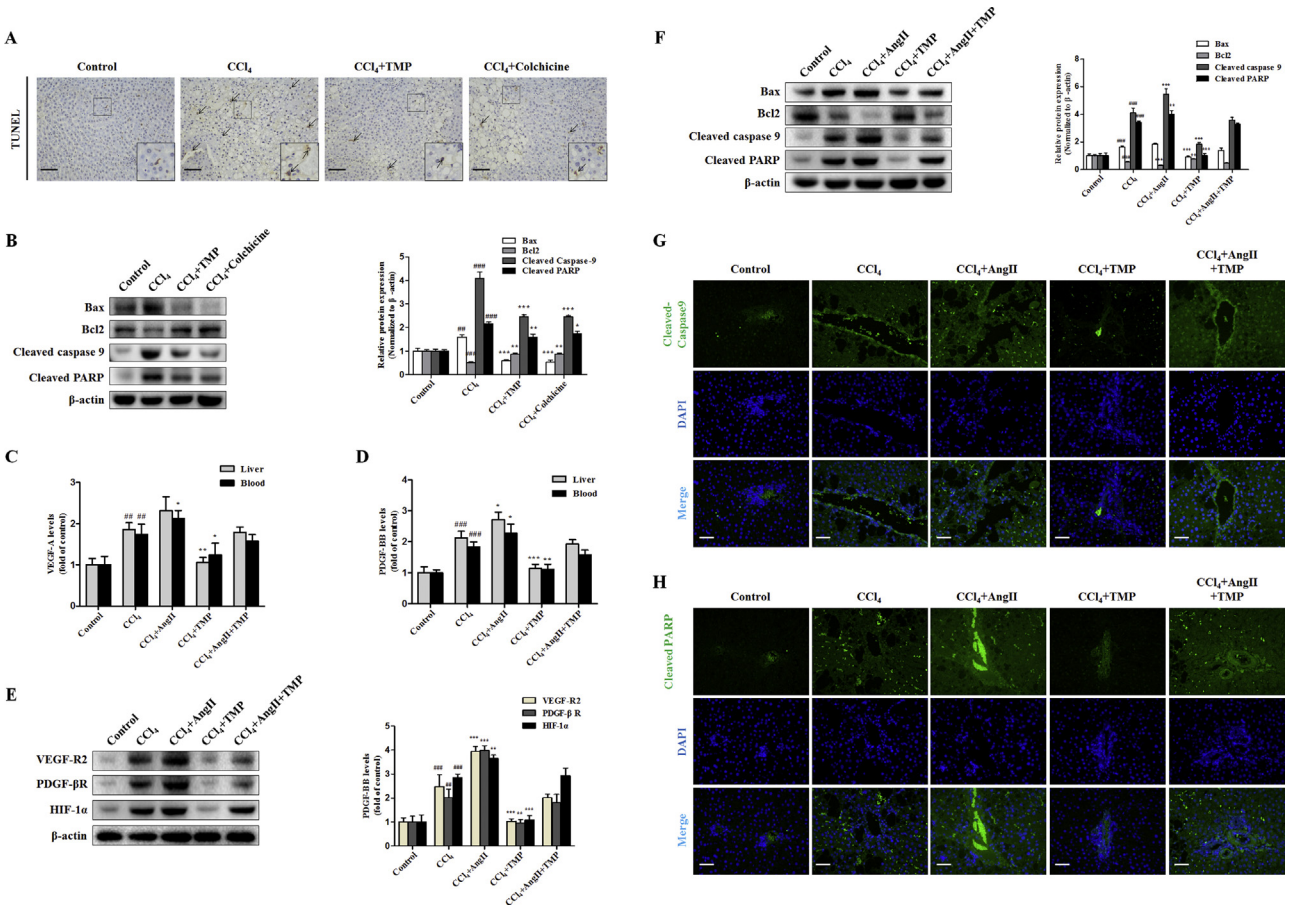

Fig. 5. Disruption of angiogenesis is required for TMP to inhibit apoptosis in rats. (A, B) Rats were grouped as follows: control group, no CCl_4, no treatment; CCl_4 group, with CCl_4, no treatment; CCl_4 + TMP group, TMP (100 mg/kg) and CCl_4-treated group; CCl_4 + colchicine group, colchicine (0.1 mg/kg) and CCl_4-treated group. **(A)** Liver sections were subjected to TUNEL staining for evaluating apoptosis (arrow). Scale bar = 20 μm. **(B)** Western blots analyses of Bcl2, Bax, Cleaved Caspase 9 and Cleaved PARP. β-actin was used as an invariant control for equal loading. Representative blots are shown with densitometry. **(C–H)** Rats were grouped as follows: control group, no CCl_4, no treatment; CCl_4 group, with CCl_4, continuous infusion of saline with mini-Osmotic pumps, but no treatment; CCl_4 + AngII group, which rats were i.p. injected with CCl_4 and continuous infusion of AngII (25 μg/kg/h) with mini-Osmotic pumps; CCl_4 + TMP group, TMP (100 mg/kg), CCl_4 treatment and continuous infusion of saline with mini-Osmotic pumps; CCl_4 + AngII + TMP group, AngII, CCl_4-treated and TMP (100 mg/kg) group. **(C)** Determination of liver homogenate and serum VEGF-A levels. **(D)** Determination of liver tissue and serum PDGF-BB levels. **(E)** Western blots analyses of VEGF-R2, PDGF-βR, HIF-1α. β-actin was used as an invariant control for equal loading. Representative blots are shown with densitometry. **(F)** Western blots analyses of Bcl2, Bax, Cleaved Caspase 9 and Cleaved PARP. β-actin was used as an invariant control for equal loading. Representative blots are shown with densitometry. **(G, H)** Liver sections were stained with immunofluorescence by using antibodies against Cleaved Caspase 9, Cleaved PARP. Representative photographs are shown. Scale bar = 20 μm. Data are expressed as mean ± SD (n = 8/group); $^{\#}p < 0.05$ versus control group, $^{\#\#}p < 0.01$ versus control group, $^{\#\#\#}p < 0.001$ versus control group, $^{*}p < 0.05$ versus CCl_4 group, $^{**}p < 0.01$ versus CCl_4 group, $^{***}p < 0.001$ versus CCl_4 group.

ascites, hepatic encephalopathy, portopulmonary hypertension and hepatopulmonary syndrome [28,29].

Recent studies indicated that angiogenesis was associated with hepatic fibrosis of different etiologies. Metabolism of CCl_4 in the liver results in stimulation of hypoxia in liver, which can initiate the process of angiogenesis [30]. In present study, we confirmed the enhanced angiogenesis in the CCl_4-induced liver injured demonstrated by significantly increased PDGF-BB and VEGF-A levels. However, TMP markedly abolished the increase of PDGF-BB and VEGF-A levels in the rat liver, indicating the attenuation of angiogenesis. Moreover, angiogenesis may represent a direct or indirect pro-fibrogenic stimulus for LSEC capillarization [4]. Signs of angiogenesis are concomitant or precede LSEC capillarization, including fenestrate disappearing and formation of an organized basement membrane [2]. There was evidence that exposure of cultured rat LSEC to pro-angiogenesis systems or to medium containing products released from hepatocytes undergoing angiogenesis was followed by increased VEGF expression and synthesis [31].

LSEC capillarization is the pivotal event during liver angiogenesis, because capillarized LSEC are the primary source of PDGF and other pro-angiogenesis components. The process of LSEC capillarization is accompanied by upregulated expression of a series of marker proteins [32]. Our data demonstrated that TMP effectively downregulated the expression CD31, CD34, and vWF at protein levels in rat fibrotic liver. This also indicated that attenuation of liver injury by TMP was concomitant with the diminished amount of capillarized LSEC *in vivo*. Reduction in capillarized LSEC could thereby result in increased of fenestration. On the other hand, capillarization of LSEC is triggered by various cytokines and chemokines, including the pro-angiogenesis factor TGF-β and the potent mitogens PDGF and EGF, released from activated HSC, hepatocyte, and macrophage [33]. The process of LSEC capillarization is associated with upregulation of corresponding receptors, including VEGF-R2, PDGF-βR, and EGFR. Our current results showed that TMP suppressed the expression of these pro-fibrogenic receptors in the CCl_4 rat model demonstrated by real time-PCR and western blot assay. These data suggested that TMP

could interrupt VEGF-R2 and PDGF-βR pathways, resulting in inhibition of LSEC capillarization *in vivo*. Furthermore, many studies have demonstrated that HGF expression was transcriptionally regulated by these pro-angiogenesis cascades in LSEC [34]. It therefore could be presumed that TMP-induced reduction of HGF production was at least partially attributed to the interruption of these cascades, contributing to the anti-angiogenic efficacy.

Apoptosis is a type of programmed cell death that is characterized by cell membrane blebbing, cell shrinkage, nuclear fragmentation, chromatin condensation, and chromosomal DNA fragmentation [35]. A number of clinical, preclinical and post-mortem studies have reported that apoptotic pathways were activated in liver fibrosis [36]. We herein demonstrated that TMP up-regulated anti-apoptotic factor Bcl-2 while down-regulated of the pro-apoptotic factor Bax. In addition, TMP decreased the expressions of Cleaved Caspase-9 and Cleaved PARP. Collectively, apoptosis played a pivotal role in the protective effect of TMP on hepatic fibrosis.

In summary, our current study showed that TMP protected the rat liver from CCl_4-caused injury, angiogenesis and fibrogenesis *in vivo*. These effects could be associated with inhibition of LSEC capillarization and attenuation of hepatic apoptosis. These data collectively suggested that TMP as a natural anti-angiogenic candidate and strengthened the role of Chuanxiong as a beneficial medicine for prevention of liver fibrosis.

Conflict of interest

The Author(s) declare(s) that they have no conflicts of interest to disclose.

Acknowledgments

This work also was supported by the National Natural Science Foundation of China (81270514, 31401210), the Open Project Program of Jiangsu Key Laboratory for Pharmacology and Safety Evaluation of Chinese Materia Medica (No. JKLPSE 201502), the Project of the Priority Academic Program Development of Jiangsu Higher Education Institutions (PAPD), the Youth Natural Science Foundation of Jiangsu Province (BK20140955), the Natural Science Research General Program of Jiangsu Higher Education Institutions (14KJB310011), the Youth Natural Science Foundation of Nanjing University of Chinese Medicine (13XZR20), the project funded by the Priority Academic Pro-gram Development of Jiangsu Higher Education Institutions (ysxk-2010), and the 2013 Program for Excellent Scientific and Technological Innovation Team of Jiangsu Higher Education.

References

[1] C. Kantari-Mimoun, M. Castells, R. Klose, A.K. Meinecke, U.J. Lemberger, P.E. Rautou, H. Pinot-Roussel, C. Badoual, K. Schrödter, C.H. Österreicher, J. Fandrey, C. Stockmann, Resolution of liver fibrosis requires myeloid cell-driven sinusoidal angiogenesis, Hepatology 61 (2015) 2042–2055.
[2] L.D. DeLeve, Liver sinusoidal endothelial cells in hepatic fibrosis, Hepatology 61 (2015) 1740–1746.
[3] S.S. Bale, S. Geerts, R. Jindal, M.L. Yarmush, Isolation and co-culture of rat parenchymal and non-parenchymal liver cells to evaluate cellular interactions and response, Sci. Rep. 6 (2016) 25329–25339.
[4] G. Xie, S.S. Choi, W.K. Syn, G.A. Michelotti, M. Swiderska, G. Karaca, I.S. Chan, Y. Chen, A.M. Diehl, Hedgehog signalling regulates liver sinusoidal endothelial cell capillarisation, Gut 62 (2013) 299–309.
[5] M.M. Tropea, B.J. Harper, G.M. Graninger, T.M. Phillips, G. Ferreyra, H.S. Mostowski, R.L. Danner, A.F. Suffredini, M.A. Solomon, Isolation of a circulating CD45-, CD34dim cell population and validation of their endothelial phenotype, Thromb. Haemost. 112 (2014) 770–780.
[6] S.M. Raines, O.C. Richards, L.R. Schneider, K.L. Schueler, M.E. Rabaglia, A.T. Oler, D.S. Stapleton, G. Genové, J.A. Dawson, C. Betsholtz, A.D. Attie, Loss of PDGF-B activity increases hepatic vascular permeability and enhances insulin sensitivity, Am. J. Physiol. Endocrinol. Metab. 301 (2011) E517–E526.
[7] F. Zhang, Z.L. Zhang, L. Chen, D.S. Kong, X.P. Zhang, C.F. Lu, Y. Lu, S. Zheng, Curcumin attenuates angiogenesis in liver fibrosis and inhibits angiogenic properties of hepatic stellate cells, J. Cell Mol. Med. 18 (2014) 1392–1406.
[8] Z. Yan, K. Qu, J. Zhang, Q. Huang, P. Qu, X. Xu, P. Yuan, X. Huang, Y. Shao, Liu, H. Zhang, J. Xing, CD147 promotes liver fibrosis progression via VEGF-A/VEGFR2 signalling-mediated cross-talk between hepatocytes and sinusoidal endothelial cells, Clin. Sci. (Lond.) 129 (2015) 699–710.
[9] W.S. Moon, H.S. Park, K.H. Yu, M.Y. Park, K.R. Kim, K.Y. Jang, J.S. Kim, B.H. Cho, Expression of betacellulin and epidermal growth factor receptor in hepatocellular carcinoma: implications for angiogenesis, Hum. Pathol. 37 (2006) 1324–1332.
[10] S.M. Yeligar, K. Machida, H. Tsukamoto, V.K. Kalra, Ethanol augments RANTES/CCL5 expression in rat liver sinusoidal endothelial cells and human endothelial cells via activation of NF-kappa B, HIF-1 alpha, and AP-1, J. Immunol. 183 (2009) 5964–5976.
[11] H. Li, C. Zhang, R. Fan, S. Hua, H. Xie, J. Luo, Y. Wang, H. Lv, T. Tang, The effects of Chuanxiong on the pharmacokinetics of warfarin in rats after biliary drainage, J. Ethnopharmacol. (2016) 30525–33526 (pii: S0378-8741).
[12] Y.L. Lin, Y.C. Hsu, Y.T. Chiu, Y.T. Huang, Antifibrotic effects of a herbal combination regimen on hepatic fibrotic rats, Phytother. Res. 22 (2008) 69–76.
[13] W.J. Zhang, P. Wang, M.J. Yang, Y.G. Wang, Y. Ju, R.H. Du, Analyze and compare activities of polysaccharide form rhizoma chuanxiong and radix paeoniae rubra, Zhong Yao Cai 34 (2011) 1569–1574.
[14] C.M. Li, J.H. Wu, R.F. Yang, X.L. Dong, Z.Y. He, X.L. Tian, D.J. Guo, M.S. Wong, T.Q. Qiu, S.W. Chan, Ligusticum chuanxiong prevents ovariectomy-induced liver and vascular damage in rats, Am. J. Chin. Med. 41 (2013) 831–848.
[15] X.F. Wu, F. Zhang, X. Xiong, C.F. Lu, N.Q. Lian, Y. Lu, S.Z. Zheng, Tetramethylpyrazine reduces inflammation in liver fibrosis and inhibits inflammatory cytokine expression in hepatic stellate cells by modulating NLRP3 inflammasome pathway, IUBMB Life 67 (2015) 312–321.
[16] M. Miyao, H. Kotani, T. Ishida, C. Kawai, S. Manabe, H. Abiru, K. Tamaki, Pivotal role of liver sinusoidal endothelial cells in NAFLD/NASH progression, Lab. Invest. 95 (2015) 1130–1144.
[17] Y. Taga, M. Kusubata, K. Ogawa-Goto, S. Hattori, Developmental stage-dependent regulation of prolyl 3-Hydroxylation in tendon type I collagen, J. Biol. Chem. 291 (2016) 837–847.
[18] L. Guo, A.H. Wang, Y.L. Sun, C.G. Xu, Evaluation of antioxidant and immunity function of tetramethylpyrazine phosphate tablets in vivo, Molecules 17 (2012) 5412–5421.
[19] Y. Ding, X.F. Hou, L. Chen, H. Zhou, Y.J. Gong, L.Q. Dai, Y. Zheng, Heme oxygenase-1 dependant pathway contributes to protection by tetramethylpyrazine against chronic hypoxic injury on medulla oblongata in rats, J. Neurol. Sci. 361 (2016) 101–111.
[20] X.W. Che, Y. Zhang, H. Wang, W. Wang, Effect of ligustrazine injection on levels of interleukin-4 and interferon-gamma in patients with bronchial asthma, Chin. J. Integr. Med. 14 (2008) 217–220.
[21] A. Page, P. Paoli, E. Moran Salvador, S. White, J. French, J. Mann, Hepatic stellate cell transdifferentiation involves genome-wide remodeling of the DNA methylation landscape, J. Hepatol. 64 (2016) 661–673.
[22] F. Zhang, D.S. Kong, Z.L. Zhang, N. Lei, X.J. Zhu, X.P. Zhang, L. Chen, S.Z. Lu, Tetramethylpyrazine induces G0/G1 cell cycle arrest and stimulates mitochondrial-mediated and caspase-dependent apoptosis through modulating ERK/p53 signaling in hepatic stellate cells in vitro, Apoptosis 18 (2013) 135–149.
[23] Y.L. Lin, Y.C. Hsu, Y.T. Chiu, Y.T. Huang, Antifibrotic effects of a herbal combination regimen on hepatic fibrotic rats, Phytother. Res. 22 (2008) 69–76.
[24] K.F. Zhang, Y. Gao, M.L. Zhong, Y. Xu, J. Li, Y. Chen, X. Duan, H. Zhu, Hepatoprotective effects of Dicliptera chinensis polysaccharides on dimethylnitrosamine-induced hepatic fibrosis rats and its underlying mechanism, J. Ethnopharmacol. 179 (2016) 38–44.
[25] X.J. Zhu, F. Zhang, L. Zhou, D. Kong, L. Chen, Y. Lu, S. Zheng, Diallyl trisulfide attenuates carbon tetrachloride-caused liver injury and fibrogenesis and reduces hepaticoxidative stress in rats, Naunyn Schmiedebergs Arch. Pharmacol. 387 (2014) 445–455.
[26] D.S. Guan, Y.F. Su, Y.X. Li, C.J. Wu, Y. Meng, X. Peng, Y.L. Cui, Tetramethylpyrazine inhibits CoCl2 −induced neurotoxicity through enhancement of Nrf2/GCLc/GSH and suppression of HIF1α/NOX2/ROS pathways, J. Neurochem. 134 (2015) 551–565.
[27] X.C. Sun, L.X. Sun, X.J. Shi, S.J. Kang, Ligustrazine fought against cisplatin induced ototoxicity in guinea pigs, Zhongguo Zhong Xi Yi Jie He Za Zhi 34 (2014) 982–986.
[28] V. Calderone, J. Gallego, G. Fernandez-Miranda, E. Garcia-Pras, C. Maillo, A. Berzigotti, M. Mejias, F.A. Bava, A. Angulo-Urarte, M. Graupera, P. Navarro, J. Bosch, M. Fernandez, R. Mendez, Sequential functions of CPEB1 and CPEB4 regulate pathologic expression of vascular endothelial growth factor and angiogenesis in chronic liver disease, Gastroenterology 150 (2016) 982–997.
[29] J.C. Gana, C.A. Serrano, S.C. Ling, Angiogenesis and portal-systemic collaterals in portal hypertension, Ann. Hepatol. 15 (2016) 303–313.
[30] Y.N. Zhou, Y.P. Mu, W.W. Fu, B.B. Ning, G.L. Du, J.M. Chen, M.Y. Sun, H. Zhang, Y.Y. Hu, C.H. Liu, L.M. Xu, P. Liu, Yiguanjian decoction and its ingredients inhibit angiogenesis in carbon tetrachloride-induced cirrhosis mice, BMC Complement. Altern. Med. 15 (2015) 342–351.
[31] I. Arutyunyan, T. Fatkhudinov, E. Kananykhina, N. Usman, A. Elchaninov, A. Makarov, G. Bolshakova, D. Goldshtein, G. Sukhikh, stromal/stem cells: in vitro study, Stem Cell Res. Ther. 7 (2016) 46–59.

[32] N. Pascuali, L. Scotti, D. Abramovich, G. Irusta, M. Di Pietro, D. Bas, M. Tesone, F. Parborell, Inhibition of platelet-derived growth factor (PDGF) receptor affects follicular development and ovarian proliferation, apoptosis and angiogenesis in prepubertal eCG-treated rats, Mol. Cell Endocrinol. 412 (2015) 148–158.
[33] K. Sakata, S. Eda, E.S. Lee, M. Hara, M. Imoto, S. Kojima, Neovessel formation promotes liver fibrosis via providing latent transforming growth factor-β, Biochem. Biophys. Res. Commun. 443 (2014) 950–956.
[34] G. Marrone, V.H. Shah, J. Gracia-Sancho, Sinusoidal communication in liver fibrosis and regeneration, J. Hepatol. 65 (2016) 608–617.
[35] I.A. Darby, N. Zakuan, F. Billet, A. Desmoulière, The myofibroblast, a key cell in normal and pathological tissue repair, Cell Mol. Life Sci. 73 (2016) 1145–1157.
[36] R. Weiskirchen, F. Tacke, Liver fibrosis: from pathogenesis to novel therapies, Dig. Dis. 34 (2016) 410–422.